

# TWO-DIMENSIONAL STATISTICAL TEST FOR THE PRESENCE OF ALMOST CYCLOSTATIONARITY ON IMAGES

*David Vázquez-Padín<sup>1</sup>, Carlos Mosquera<sup>1</sup> and Fernando Pérez-González<sup>1,2</sup>*

1. Signal Theory and Communications Department, University of Vigo, Vigo 36310

2. Electrical and Computer Engineering Department, University of New Mexico, Albuquerque, NM

## ABSTRACT

In this work, we study the presence of almost cyclostationary fields in images for the detection and estimation of digital forgeries. The almost periodically correlated fields in the two-dimensional space are introduced by the necessary interpolation operation associated with the applied spatial transformation. In this theoretical context, we extend a statistical time-domain test for presence of cyclostationarity to the two-dimensional space.

The proposed method allows us to estimate the scaling factor and the rotation angle of resized and rotated images, respectively. Examples of the output of our method are shown and comparative results are presented to evaluate the performance of the two-dimensional extension.

**Index Terms**— Image forensics, spatial transformation, cyclostationarity, interpolation, resampling factor estimation

## 1. INTRODUCTION

Nowadays, there are a lot of powerful and intuitive image editing tools that facilitate the manipulation and alteration of digital images. With the aim of identifying the type of forgery, several blind (or passive) techniques have been proposed in the past few years. When an image forgery is carried out, most of the time it is necessary to perform geometric transformations like scaling, rotation or skewing.

The detection of these spatial transformations has been studied in [1] and [2]. The former uses an expectation-maximization (EM) algorithm to detect periodic patterns and then expose forgeries, but the main problem lies in the correct initialization of the parameters for the EM convergence. The latter is based on a derivative operator and Radon transformation that provides a blind and very fast method capable of detecting traces of spatial transformations, but presents some weaknesses in the estimation of the rotation angle and scaling factor, due to the one-dimensional approach.

Motivated by these shortcomings and the need of a theoretical framework to explain why the interpolated images present a periodically correlated field, we propose to use the cyclostationarity theory for the estimation of the resampling factor. The method that we propose is a two-dimensional extension of a statistical time-domain test proposed by Dandawáté and Giannakis in [3], allowing us to estimate the resampling factor of a spatially transformed image, specifically the scaling factor and the rotation angle.

This work was partially funded by Xunta de Galicia under Projects 07TIC012322PR (FACTICA), 2006/150 (Consolidation of Research Units), by the Spanish Ministry of Science and Innovation under projects COMONSENS (ref. CSD2008-00010) and SPROACTIVE (ref. TEC2007-68094-C02-01/TCM) and by the Prince of Asturias Chair in Information Science and Related Technologies.

In the next section, we present the notation and the model used for the spatial transformation of images and then we introduce the cyclostationarity theory needed for the estimation of the resampling factor. In Section 3, we explain the extension of the time-domain test for presence of cyclostationarity to the two-dimensional space. Section 4 presents the results obtained with our method comparing those obtained with the method of Mahdian and Saic [2]. Finally, Section 5, provides the conclusions and further work.

## 2. PRELIMINARIES AND PROBLEM STATEMENT

Throughout the paper we will consider an original image as the output provided by an acquisition system after the operations of sampling and quantization. The resulting digital image  $f(x_1, x_2)$  is a matrix of integer values (gray levels) defined on a discrete grid of size  $N_1 \times N_2$ . The convention used for the coordinates  $(x_1, x_2)$  is that  $x_1 \in \{0, \dots, N_1 - 1\}$  represents the horizontal axis and  $x_2 \in \{0, \dots, N_2 - 1\}$  represents the vertical axis. We will denote vectors and matrices by bold letters, for example  $\mathbf{x} = (x_1, x_2)$ .

### 2.1. Spatial Transformations

The spatial transformation of an original image  $f(x_1, x_2)$  maps the intensity value at each pixel location  $(x_1, x_2)$  to another location  $(y_1, y_2)$  in the new image  $g(y_1, y_2)$ . The most commonly used is the affine transformation that combines several linear operations like translation, rotation, scaling, skewing, etc. The mapping can be expressed as:

$$\begin{bmatrix} y_1 \\ y_2 \end{bmatrix} = \mathbf{A} \begin{bmatrix} x_1 \\ x_2 \end{bmatrix} + \mathbf{b},$$

where  $\mathbf{A}$  is the matrix that defines the linear transformation and  $\mathbf{b}$  represents the translation vector. In general, the pixels in the resulting image will not map to exact integer coordinates on the source image, but rather to intermediate locations between source pixels. Therefore, when we perform any of the mentioned spatial transformations we need to make use of a pixel interpolation algorithm. The interpolation of a spatial transformed image  $f(y_1, y_2)$  by a resampling factor  $N_s = (N_{s1}, N_{s2}) = (L_1/M_1, L_2/M_2)$  can be modeled by the following expression:

$$g(x_1, x_2) = \sum_{i=-\infty}^{\infty} \sum_{j=-\infty}^{\infty} f(i, j) h(x_1 M_1 - i L_1, x_2 M_2 - j L_2), \quad (1)$$

where  $g(x_1, x_2)$  is the resampled image and  $h(x_1, x_2)$  represents the interpolation kernel. Many different interpolation filters are available with different characteristics, but the most common are the nearest neighbor, linear, cubic and truncated sinc.

## 2.2. Cyclostationary approach

Once we have mathematically described the resampling process we can observe from (1), that an interpolated image can be seen as a random field  $f(x_1, x_2)$  (the original image) that is periodically filtered with the same kernel  $h(x_1, x_2)$ . Therefore, the resampled image will exhibit periodically correlated fields (cf. [4]) with a period equal to the resampling factor  $N_s = (L_1/M_1, L_2/M_2)$ . Equivalently, the output image is cyclostationary with period  $N_s$ .

In the one-dimensional case, Sathe and Vaidyanathan showed in [5] that the output of a multirate system that performs sampling rate conversion by a factor  $N_s = L/M$ , produces a cyclostationary signal with period  $L/\gcd(L, M)$  if the input signal is wide sense stationary (the output becomes wide sense stationary only if the interpolation filter is ideal). They only consider pure cyclostationary processes, i.e. with an integer cyclic period; nevertheless, for the estimation of the resampling factor it is more convenient to consider that the output can be an almost cyclostationary process.

This idea regarding multirate systems can be extended to the spatial domain with two dimensions, but before we have to extend the concept of almost cyclostationarity to the two-dimensional space. As it is mentioned in [6], those time series that have an “almost integer” period accept generalized (or limiting) Fourier expansions, so following the definition in [4] of periodically correlated fields with an integer period, we introduce the concept of almost cyclostationary random fields.

**Definition 1** Let  $x(\mathbf{m}) = x(m_1, m_2)$  be a real random field with mean  $\mu_x(\mathbf{m}) \doteq E\{x(\mathbf{m})\}$  and covariance  $c_{xx}(\mathbf{m}; \boldsymbol{\tau}) \doteq E\{[x(\mathbf{m}) - \mu_x(\mathbf{m})][x(\mathbf{m} + \boldsymbol{\tau}) - \mu_x(\mathbf{m} + \boldsymbol{\tau})]\}$ , where  $\boldsymbol{\tau} \doteq (\tau_1, \tau_2)$ . The random field  $x(m_1, m_2)$  is strongly almost periodically correlated (equivalently, almost cyclostationary) with period  $\mathbf{T} \doteq (T_1, T_2)$ , if and only if its mean and covariance functions satisfy

$$\begin{aligned}\mu_x(m_1, m_2) &= \mu_x(m_1 + kT_1, m_2 + lT_2) \\ c_{xx}((m_1, m_2); \boldsymbol{\tau}) &= c_{xx}((m_1 + kT_1, m_2 + lT_2); \boldsymbol{\tau})\end{aligned}$$

for all integers  $m_1, m_2, \tau_1, \tau_2, k, l$  and rational numbers  $T_1, T_2$ .

Such random fields accept generalized Fourier expansions and considering that  $x(m_1, m_2)$  has zero mean, the generalized Fourier series pair for every  $\boldsymbol{\tau}$  is:

$$\begin{aligned}c_{xx}(\mathbf{m}; \boldsymbol{\tau}) &= \sum_{\boldsymbol{\alpha} \in \mathcal{A}_{xx}} C_{xx}(\boldsymbol{\alpha}; \boldsymbol{\tau}) e^{j(\alpha_1 m_1 + \alpha_2 m_2)} \\ C_{xx}(\boldsymbol{\alpha}; \boldsymbol{\tau}) &= \lim_{M_1, M_2 \rightarrow \infty} \frac{1}{M_1 M_2} \sum_{m_1=0}^{M_1-1} \sum_{m_2=0}^{M_2-1} c_{xx}(\mathbf{m}; \boldsymbol{\tau}) \\ &\quad \times e^{-j(\alpha_1 m_1 + \alpha_2 m_2)},\end{aligned}\quad (2)$$

where  $\boldsymbol{\alpha} = (\alpha_1, \alpha_2)$  represents each frequency pair in the cyclic domain. The set of cyclic frequencies  $\mathcal{A}_{xx} \doteq \{\boldsymbol{\alpha} : C_{xx}(\boldsymbol{\alpha}; \boldsymbol{\tau}) \neq 0, -\pi < \alpha_1, \alpha_2 \leq \pi\}$  must be countable and we assume that the limit exists in the mean-square sense. To express those random fields in terms of the Fourier Transforms, we define the cyclic spectrum.

**Definition 2** The cyclic spectrum for random fields  $x(m_1, m_2)$ , is defined as:

$$S_{xx}(\boldsymbol{\alpha}; \boldsymbol{\omega}) \doteq \sum_{\tau_1=-\infty}^{\infty} \sum_{\tau_2=-\infty}^{\infty} C_{xx}(\boldsymbol{\alpha}; \boldsymbol{\tau}) e^{-j(\omega_1 \tau_1 + \omega_2 \tau_2)},$$

where  $\boldsymbol{\omega} = (\omega_1, \omega_2)$  represents each frequency pair in the frequency domain.

In order to show the presence of almost cyclostationary fields in a resampled image by a rational factor  $N_s$ , we consider the single case when the original image is a Gaussian field with zero mean and variance equal to one. In this situation the cyclic correlation is

$$\begin{aligned}c_{xx}(\mathbf{m}; \boldsymbol{\tau}) &= \sum_{i=-\infty}^{\infty} \sum_{j=-\infty}^{\infty} h(m_1 M_1 - i L_1, m_2 M_2 - j L_2) \\ &\quad \times h((m_1 + \tau_1) M_1 - i L_1, (m_2 + \tau_2) M_2 - j L_2)\end{aligned}$$

and it is easy to see that

$$c_{xx}((m_1, m_2); \boldsymbol{\tau}) = c_{xx}((m_1 + kL_1/M_1, m_2 + lL_2/M_2); \boldsymbol{\tau})$$

with  $k, l \in \mathbb{Z}$ . Hence, unless the kernel used is ideal, the output is almost cyclostationary with period  $\mathbf{T} = (L_1/M_1, L_2/M_2)$ . The same is true for real images having an unknown distribution which makes more difficult the estimation of the cyclic period. For this reason, we choose to extend the time-domain test proposed by Dandawaté and Giannakis in [3] that allows the detection of almost periodicities without considering a specific distribution on the data.

## 3. EXTENSION OF THE TIME-DOMAIN TEST

The calculation of the scaling factor  $N_s$  or the rotation angle  $\theta$  of a spatially transformed image can be achieved through the estimation of the cyclic frequencies  $\boldsymbol{\alpha}$ , as we will see at the end of this section. For an image block  $x(m_1, m_2)$  of size  $N \times N$  and with zero mean, the detection of the set of cyclic frequency pairs in (2) can be made through the estimation of the cyclic correlation:

$$\hat{C}_{xx}(\boldsymbol{\alpha}; \boldsymbol{\tau}) = \frac{1}{N^2} \sum_{m_1, m_2=0}^{N-1} x(\mathbf{m}) x(\mathbf{m} + \boldsymbol{\tau}) e^{-j(\alpha_1 m_1 + \alpha_2 m_2)}.\quad (3)$$

This estimate is asymptotically unbiased according to Definition 1. Thus, if we represent  $e_{xx}(\boldsymbol{\alpha}; \boldsymbol{\tau})$  as the estimation error and  $C_{xx}(\boldsymbol{\alpha}; \boldsymbol{\tau})$  as the ideal covariance, the estimation provides:

$$\hat{C}_{xx}(\boldsymbol{\alpha}; \boldsymbol{\tau}) = C_{xx}(\boldsymbol{\alpha}; \boldsymbol{\tau}) + e_{xx}(\boldsymbol{\alpha}; \boldsymbol{\tau})$$

where  $e_{xx}(\boldsymbol{\alpha}; \boldsymbol{\tau})$  vanishes asymptotically as  $N \rightarrow \infty$ . To make a decision about the presence or absence of a given cyclic frequency in the image block, we build up a vector from  $\hat{C}_{xx}(\boldsymbol{\alpha}; \boldsymbol{\tau})$  evaluated in a set of  $K$  lags  $\{\boldsymbol{\tau}_k\}_{k=1}^K = \{\boldsymbol{\tau}_1, \dots, \boldsymbol{\tau}_K : \boldsymbol{\tau}_k = (\tau_{k1}, \tau_{k2}) \in \mathbb{Z}^2\}$ :

$$\begin{aligned}\hat{\mathbf{c}}_{xx} &= \frac{1}{\sqrt{2}} \left[ \hat{C}_{xx}(\boldsymbol{\alpha}; \boldsymbol{\tau}_1), \dots, \hat{C}_{xx}(\boldsymbol{\alpha}; \boldsymbol{\tau}_K), \right. \\ &\quad \left. \hat{C}_{xx}^*(\boldsymbol{\alpha}; \boldsymbol{\tau}_1), \dots, \hat{C}_{xx}^*(\boldsymbol{\alpha}; \boldsymbol{\tau}_K) \right]^T,\end{aligned}$$

and we consider the following hypothesis testing problem:

$$\begin{aligned}\mathcal{H}_0 : \boldsymbol{\alpha} \notin \mathcal{A}_{xx}, \forall \{\boldsymbol{\tau}_k\}_{k=1}^K &\Rightarrow \hat{\mathbf{c}}_{xx} = \mathbf{e}_{xx} \\ \mathcal{H}_1 : \boldsymbol{\alpha} \in \mathcal{A}_{xx}, \text{ for some } \{\boldsymbol{\tau}_k\}_{k=1}^K &\Rightarrow \hat{\mathbf{c}}_{xx} = \mathbf{c}_{xx} + \mathbf{e}_{xx}.\end{aligned}\quad (4)$$

Note that  $\mathbf{c}_{xx}$  is the corresponding true value of the cyclic correlation vector and  $\mathbf{e}_{xx}$  is the estimation error vector. From (4), if we know the distribution of the estimation error  $\mathbf{e}_{xx}$ , we can seek a threshold to detect the cyclic frequency pairs  $(\alpha_1, \alpha_2)$  given that  $\mathbf{c}_{xx}$  is deterministic. Dandawaté and Giannakis use the asymptotic properties of the cyclic correlation estimator to infer the asymptotic distribution of the estimation error. In our case, considering that the extension to the spatial domain of the mixing conditions (A1 in [3]) is fulfilled, then

the cyclic correlation estimator in (3) is asymptotically normal and thus the error estimation converges in distribution to a multivariate normal, i.e.

$$\lim_{N \rightarrow \infty} N e_{xx} \stackrel{D}{=} \mathcal{N}(\mathbf{0}, \Sigma_{xx}),$$

where  $\mathcal{N}$  represents a multivariate normal density and  $\Sigma_{xx}$  is the asymptotic covariance matrix, which is defined as follows:

$$\begin{aligned} \Sigma_{xx} &\doteq \lim_{N \rightarrow \infty} N^2 \text{cov}\{\hat{c}_{xx}, \hat{c}_{xx}^H\} \\ &= \frac{1}{2} \begin{bmatrix} \mathbf{S}_{\tau_k, \tau_l}^{(*)}(\mathbf{0}; -\alpha) & \mathbf{S}_{\tau_k, \tau_l}(2\alpha; \alpha) \\ (\mathbf{S}_{\tau_k, \tau_l}(2\alpha; \alpha))^* & (\mathbf{S}_{\tau_k, \tau_l}^{(*)}(\mathbf{0}; -\alpha))^* \end{bmatrix}. \end{aligned}$$

In the above expression,  $\mathbf{S}_{\tau_k, \tau_l}(\alpha, \omega)$  is a  $K \times K$  matrix whose  $(k, l)^{\text{th}}$  entries are given by the cyclic cross-spectrum of  $y(\mathbf{m}; \tau_k) \doteq x(\mathbf{m})x(\mathbf{m} + \tau_k)$  and  $y(\mathbf{m}; \tau_l) \doteq x(\mathbf{m})x(\mathbf{m} + \tau_l)$  for the different  $K$  lags and, on the other hand, the matrix  $\mathbf{S}_{\tau_k, \tau_l}^{(*)}(\alpha, \omega)$  is composed by the cyclic cross-spectrum of  $y(\mathbf{m}; \tau_k)$  and  $y^*(\mathbf{m}; \tau_l)$ . Hence, for  $N$  large enough, the vector  $\hat{c}_{xx}$  under  $\mathcal{H}_0$  and  $\mathcal{H}_1$  differs only in the mean. In order to solve this detection problem, we use (in the same way as in [3]) the norm of a weighted version of the cyclic correlation estimation vector ( $\gamma = N \hat{c}_{xx}^H \hat{\Sigma}_{xx}^{-1/2}$ ), so the statistic and then the likelihood ratio test with a threshold  $\Gamma$  correspond to:

$$\mathcal{T}_{xx} = \|\gamma\|^2 = N^2 \hat{c}_{xx}^H \hat{\Sigma}_{xx}^{-1} \hat{c}_{xx} \underset{\mathcal{H}_0}{\overset{\mathcal{H}_1}{\geq}} \Gamma,$$

where  $\hat{\Sigma}_{xx}$  is an estimate of the asymptotic covariance matrix. From Theorem 2 in [3], the statistic  $\mathcal{T}_{xx}$  has the following asymptotic distribution under  $\mathcal{H}_0$

$$\lim_{N \rightarrow \infty} \mathcal{T}_{xx} \stackrel{D}{=} \chi_{2K}^2$$

where  $\chi_{2K}^2$  represents a chi-square distribution with  $2K$  degrees of freedom. Under  $\mathcal{H}_1$  and for  $N$  large enough, the asymptotic distribution is approximately Gaussian

$$\mathcal{T}_{xx} \sim \mathcal{N}(N^2 \hat{c}_{xx}^H \hat{\Sigma}_{xx}^{-1} \hat{c}_{xx}, 4N^2 \hat{c}_{xx}^H \hat{\Sigma}_{xx}^{-1} \hat{c}_{xx}).$$

Once we know the asymptotic distribution of the statistic  $\mathcal{T}_{xx}$  under the two hypotheses, we can set the threshold  $\Gamma$  for a fixed probability of false alarm  $P_F = \Pr(\mathcal{T}_{xx} \geq \Gamma | \mathcal{H}_0) = \Pr(\chi_{2K}^2 \geq \Gamma)$  and then estimate the set of cyclic frequencies  $\mathcal{A}_{xx}$ . Below, the fundamental steps for the implementation of our method are presented.

After choosing an image block  $x(m_1, m_2)$  for the analysis, we apply the following algorithm for each frequency pair  $(\alpha_1, \alpha_2)$  defined in the FFT grid:

1. From the data  $x(m_1, m_2)$  and using (3), we compute the vector  $\hat{c}_{xx}$  for a fixed set of  $K$  lags  $\{\tau_k\}_{k=1}^K$ .
2. We estimate the asymptotic covariance matrix  $\Sigma_{xx}$  using the cyclic spectrum estimator. From the two options available for cyclic spectral estimation [6], we use the smoothed periodogram with a frequency domain window  $W(\omega_1, \omega_2)$  of size  $P \times P$  (with  $P$  odd). So, considering that  $F_\tau(\omega) = \sum_{m_1, m_2=0}^{N-1} x(\mathbf{m})x(\mathbf{m} + \tau)e^{-j(\omega_1 m_1 + \omega_2 m_2)}$ , then we calculate the elements of the matrix  $\hat{\Sigma}_{xx}$  as

$$\begin{aligned} &\hat{\mathbf{S}}_{\tau_k, \tau_l}^{(*)}(\mathbf{0}; -\alpha) \\ &= \frac{1}{(NP)^2} \sum_{r=-(P-1)/2}^{(P-1)/2} \sum_{s=-(P-1)/2}^{(P-1)/2} W(r, s) \\ &\times F_{\tau_k} \left( \alpha_1 + \frac{2\pi r}{N}, \alpha_2 + \frac{2\pi s}{N} \right) F_{\tau_l}^* \left( \alpha_1 + \frac{2\pi r}{N}, \alpha_2 + \frac{2\pi s}{N} \right) \end{aligned}$$

and for  $\hat{\mathbf{S}}_{\tau_k, \tau_l}(2\alpha; \alpha)$  we take the same expression used for  $\hat{\mathbf{S}}_{\tau_k, \tau_l}^{(*)}(\mathbf{0}; -\alpha)$ , but considering  $F_{\tau_l}(\omega)$  instead of  $F_{\tau_l}^*(\omega)$ .

3. We calculate the test statistic  $\mathcal{T}_{xx} = N^2 \hat{c}_{xx}^H \hat{\Sigma}_{xx}^{-1} \hat{c}_{xx}$ .
4. For a given probability of false alarm  $P_F$ , we set  $\Gamma$ .
5. We declare the frequency pair  $(\alpha_1, \alpha_2)$  as cyclic if  $\mathcal{T}_{xx} \geq \Gamma$ .

After the application of the method, we obtain the resampling factor  $N_s = (N_{s_1}, N_{s_2})$  from the detected cyclic frequencies  $(\alpha_1, \alpha_2)$ , due to the relation between these and the cyclic periods  $(T_1, T_2)$ , i.e.  $\alpha_i = 2\pi/T_i = 2\pi/N_{s_i}$  with  $i = \{1, 2\}$ . However, because of aliasing, we have the same cyclic frequencies for the scaling factors  $N_{s_i}$  and  $\frac{N_{s_i}}{N_{s_i}-1}$ . So, despite this unavoidable ambiguity, the estimated value of the resampling factor can be computed as follows:

$$\hat{N}_{s_i} = \begin{cases} \frac{2\pi}{2\pi - |\alpha_i|}, & -\pi \leq \alpha_i \leq \pi \quad (\hat{N}_{s_i} \leq 2) \\ \frac{2\pi}{|\alpha_i|}, & -\pi \leq \alpha_i \leq \pi \quad (\hat{N}_{s_i} \geq 2) \end{cases}$$

for  $i = \{1, 2\}$ . On the other hand, if we consider that  $\theta$  is the angle of rotation of the image in a counterclockwise direction around its center point, the estimation of this one from the detected cyclic frequencies  $(\alpha_1, \alpha_2)$  can be reached through the following relation:

$$\beta = \arctan\left(\frac{\alpha_2}{\alpha_1}\right) \bmod \frac{\pi}{2}$$

where mod represents the modulo operation and finally, the estimated angle is obtained by

$$\hat{\theta} = \begin{cases} -2\beta, & \text{if } 0 \leq \beta \leq \frac{\pi}{12} \\ -\arccos(\kappa), & \text{if } \frac{\pi}{12} < \beta \leq \frac{5\pi}{12} \\ \frac{\pi}{2} - 2\beta, & \text{if } \frac{5\pi}{12} < \beta \leq \frac{\pi}{2} \end{cases}$$

where  $\kappa \doteq \cos^2(\beta)(\sqrt{2 \tan(\beta)} - \tan(\beta) + \tan^2(\beta))$ . Because of the symmetry of the Discrete Fourier Transform, the cyclic frequencies for the angles  $\theta = -30$  and  $\theta = -60$  are the same and thus, there is an ambiguity when estimating these precise angles.

## 4. EXPERIMENTAL RESULTS

With the aim of showing how is the output of our method, we present in Fig. 1 the results obtained for two different spatial transformations. Figs. 1(a) and 1(d) show the analyzed block of size  $128 \times 128$  pixels in each spatially transformed image. The statistic  $\mathcal{T}_{xx}$  is plotted in Figs. 1(b) and 1(e), where we can distinguish the peaks indicating the presence of possible cyclic frequencies. In both cases, the spectral window used is a two-dimensional Kaiser window of parameter 1 with the size indicated in the caption. After using the threshold  $\Gamma$ , we represent in Figs. 1(c) and 1(f) the detected cyclic frequencies that make possible the identification of the applied transformation.

For the evaluation of our method, we use 40 TIFF format images from the miscellaneous volume of the USC-SIPI image database (we do not take into account the test pattern images) and we perform two different experiments. In order to evaluate the performance of our method, we compare our results with those obtained using the method proposed by Mahdian and Saic in [2]. Since our main objective is to detect forgeries in a relatively small region of the image, we use an image block of size  $128 \times 128$  pixels for both methods. The sizes of the tested images are of  $256 \times 256$ ,  $512 \times 512$  or  $1024 \times 1024$  pixels, so whenever possible we apply both methods to four blocks and take the average of the results obtained for each image.

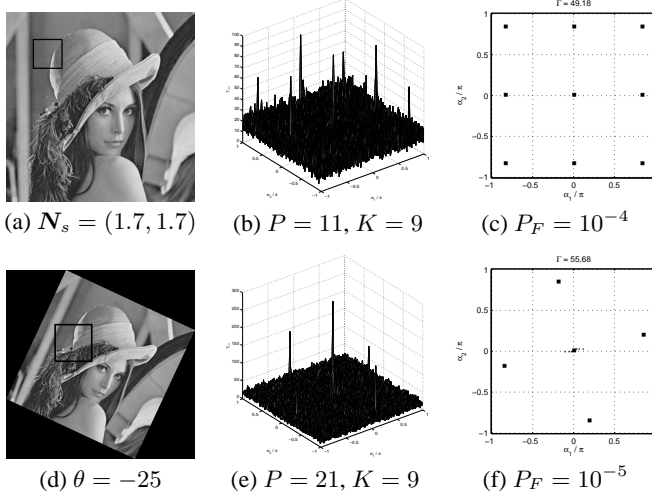


**Fig. 1.** Graphical results obtained with our method for two different spatial transformations.

In the first experiment we study the estimation accuracy for different scaling factors separated a distance of 0.05, i.e.  $N_s \in \{1.05, 1.1, \dots, 2.2, 2.25\}$ . For every value of  $N_s$ , we apply the same scaling factor for the horizontal and vertical axes of each image and use a Lanczos-3 kernel (truncated sinc) as the interpolation filter. We consider that the estimation is correct if the estimated scaling factor satisfies  $|\hat{N}_s - N_s| < 0.05$ , due to the distance between the analyzed scaling factors. In Fig. 2(a) we plot the average estimation accuracy from the 40 images for both methods in terms of percentage. We also represent the estimation accuracy of our method applying first a Laplacian operator to the whole image. As we can see the performance of our method is worse if we do not use the Laplacian prefilter, mainly for scaling factors close to 1. This is due to the use of a high pass filter like the Laplacian operator that eliminates low-frequency components, where the spectral peaks corresponding to these scaling factors are located, and this fact improves the results. It can also be observed that the method of Mahdian and Saic cannot detect the resampling factor  $N_s = 2$ , which is not an issue for our method.

In the second experiment we analyze the performance of our method when the 40 images from the database are rotated by an angle in the set  $\theta \in \{-89, -87.5, \dots, -2.5, -1\}$  (the distance between different angles is 2.5, except for the extremes). In this case, we use a bicubic interpolation kernel and consider that the estimation of the angle is correct for our method if the estimated angle satisfies  $|\hat{\theta} - \theta| < 2.5$ . For the method of Mahdian and Saic we use other criterion because we can only determine the angle from the position of the corresponding spectral peak, so in this case, we consider that the angle is correct if  $|\hat{N}_s^{(\theta)} - N_s^{(\theta)}| < 0.015$ . The threshold used in both cases is equivalent because it corresponds to the minimum distance between the theoretical values for the considered set of angles. Fig. 2(b) shows the comparative results for both methods. The best results are obtained when our method is combined with the use of a Laplacian operator. We have to notice that the output of the method of Mahdian and Saic presents the spectral peaks in the same positions for angles  $\theta$  and  $-90 - \theta$ , so  $\hat{N}_s^{(\theta)} = \hat{N}_s^{(-90-\theta)}$ . Hence, their method shows more ambiguities than ours, which just fails for  $\theta = -30$  and  $\theta = -60$ . Despite of this, the shown results are pre-

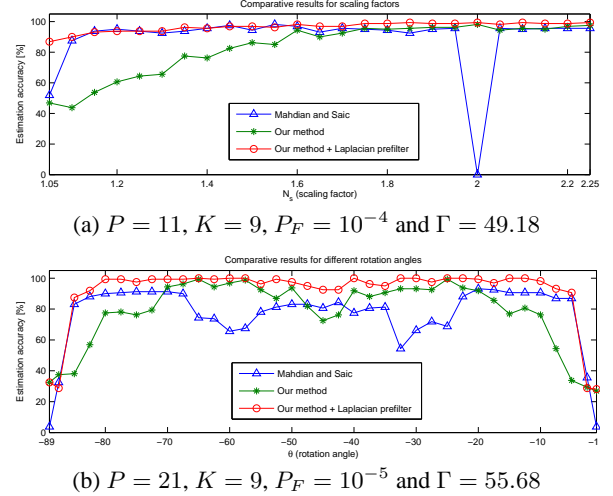


**Fig. 2.** Comparative results obtained with both methods for different scaling factors and rotation angles.

sented without considering these errors. All the experiments were carried out in Matlab.

## 5. CONCLUSIONS

We have proposed a method to estimate the parameters of spatially transformed images that performs better than the method proposed in [2]. As a counterpart, our method is more time consuming, but the processing in the two-dimensional space provides more information. For instance, we avoid some ambiguities caused by indistinguishable periodic patterns in the one-dimensional case.

Further research will focus on explaining the improvement afforded by the Laplacian prefilter. Others aspects to be studied will be the estimation of the covariance matrix, so as to get the optimum weighting matrix for the estimation of the parameters of the spatial transformations.

## 6. REFERENCES

- [1] A.C. Popescu and H. Farid, "Exposing digital forgeries by detecting traces of resampling," *IEEE Trans. on Signal Processing*, vol. 53, no. 2, pp. 758–767, Feb. 2005.
- [2] B. Mahdian and S. Saic, "Blind authentication using periodic properties of interpolation," *IEEE Trans. on Information Forensics and Security*, vol. 3, no. 3, pp. 529–538, Sept. 2008.
- [3] A.V. Dandawaté and G.B. Giannakis, "Statistical tests for presence of cyclostationarity," *IEEE Trans. on Signal Processing*, vol. 42, no. 9, pp. 2355–2369, Sept. 1994.
- [4] H. Hurd, G. Kallianpur, and J. Farshidi, "Correlation and spectral theory for periodically correlated fields indexed on  $\mathbb{Z}^2$ ," *Center for Stochastic Processes Tech Report*, vol. 448, 1997.
- [5] V.P. Sathe and P.P. Vaidyanathan, "Effects of multirate systems on the statistical properties of random signals," *IEEE Trans. on Signal Processing*, vol. 41, no. 1, pp. 131–146, Jan. 1993.
- [6] G.B. Giannakis, "Cyclostationary signal analysis," *Digital Signal Processing Handbook*, pp. 17.1–17.31, 1998.